



AIAS 2018 International Conference on Stress Analysis

# Simulation of crash events for an electric four wheel vehicle

Lorenzo Berzi<sup>a\*</sup>, Nicolò Baldanzini<sup>a</sup>, Daniele Barbani<sup>a</sup>, Massimo Delogu<sup>a</sup>, Ramses Sala<sup>ab</sup>, Marco Pierini<sup>a</sup>

<sup>a</sup>Department of Industrial Engineering, University Of Florence, Via di S.Marta 3, 50139 Firenze, Italy

<sup>b</sup>Department of Mechanical and Process Engineering, Technische Universität Kaiserslautern, Gottlieb-Daimler-Strasse 67663 Kaiserslautern

## Abstract

The diffusion of small size electric vehicles mainly designed for the urban context can significantly reduce the impact of personal mobility not only due to reduced energy consumption but also optimizing the use of parking and driving space in comparison with conventional vehicles. The solutions proposed on the market and at research level include innovations both in terms of layout (e.g. three and four wheel tilting vehicles) and in terms of powertrain, such as electric ones. The design, the sizing, the integration of battery system in vehicles are critical; this component directly determines overall performances, its mass and cost are relevant in comparison with the whole vehicle, it is subjected to ageing during use and, potentially, it can cause overheating or other failures in case of adverse events. This work is related to the analysis of a four-wheel electric vehicle mainly conceived for urban use; its size is compact and its dynamic performances are comparable to powered two wheelers due to tilting characteristics. The behaviour in case of crash is examined in order to estimate the solicitations on the battery and to verify any eventual implication on vehicle safety, at least for certain crash configuration. The activity included the definition of testing methods for electrochemical devices, a phase necessary to define the order of magnitude of acceleration events to which the single cells and/or the battery system have to be tolerant. Therefore, a full finite-element vehicle model has been defined starting from prototype vehicle design CAD, using realistic inertia and stiffness data also for battery compartment. The model has been used to simulate crash events against barrier and against other vehicles, repeating the analysis for a range of impact points and direction. The obtained estimation of deformation and acceleration values on battery system are presented.

© 2018 The Authors. Published by Elsevier B.V.

This is an open access article under the CC BY-NC-ND license (<http://creativecommons.org/licenses/by-nc-nd/3.0/>)

Peer-review under responsibility of the Scientific Committee of AIAS 2018 International Conference on Stress Analysis.

*Keywords:* Electric Vehicles; Light vehicles; Battery; Crashworthiness; Simulation; Accident.

\* Corresponding author. Tel.: +39 055 2758698

E-mail address: [lorenzo.berzi@unifi.it](mailto:lorenzo.berzi@unifi.it)

## 1. Introduction to Electric L-Vehicles

Considering the whole circulating fleet of private passenger vehicles in Europe, the diffusion of L-vehicles (two, three and four wheels light vehicles as described by Reg. 168 of the EU) and the dimension of the market is about one order of magnitude smaller in comparison with those of conventional, full-size vehicles (passenger cars up to 3,5t, defined as “M1 class”). Nevertheless, according to the increasing sensitiveness of Authorities, of users and of the whole automotive sector about sustainability, the introduction of innovative L-class small vehicles and/or microcars for urban and interurban mobility has the potential to meet users’ expectations through the modification of typical use parameters related to full size vehicle category (M1 class); suitable examples are:

- fuel/energy consumption reduction
- parking space reduction
- mitigation of traffic congestion due to overall dimension reduction
- ownership cost reduction for final user.

Similar advantages are also related to the diffusion of other types of light vehicles, such as powered cycles, which are experiencing an increasing diffusion not only in the European context but also at worldwide level (Huertas-Leyva et al., 2018). The topic has been gaining relevance in technical/scientific literature over last years; many authors described the potential growth of “urban” vehicles (Cahill et al., 2013; Cossalter et al., 2012; Festini et al., 2011) due to the opportunities for integration in modern urban contexts, which could also result in an improvement of the life quality in cities (Will et al., 2011).

Regarding the safety of electric vehicles, relevant attention is paid on the consequences of accident and crash events on the battery system, not only due to the risk of a relevant loss of economic value as a consequence of component functional failure but mainly due to the risk of potentially critical events such as overheating (Avdeev and Gilaki, 2014; Zhu et al., 2018). The present work deals with this relevant topic aiming to identify in a quantitative manner the solicitations on the battery of a prototype four wheel compact electric vehicle (L2e-class) in case of certain accidents; FEM (Finite Element Method) models are used for crash simulation.

The paper is structured as follows: the present section briefly introduces the topic. Section 2 deals with the identification of relevant accident configuration for the vehicle under examination and therefore defines the boundary conditions of the subsequent analysis. Reference solicitations on the battery are proposed starting from a brief literature study. The content of Section 3 is related to vehicle parts description and describes modeling approach. Finally, a synthesis of relevant results is presented.

## 2. Definition of vehicle characteristics and boundary conditions for crash analysis

The safety of so-called vulnerable road users (e.g. riders of cycles or of Powered Two Wheelers - PTWs) is a topic under development in research since a large potential for reduction of injuries and fatalities has been identified in case of introduction of active (Gil et al., 2017; Giovannini et al., 2014; Savino et al., 2016) or passive (Grassi et al., 2018b) safety systems. The focus of the present work is on the solicitation on vehicle and battery system in case of crash; therefore, the reduction of accident happening probability or the mitigation of the effects of the crash event are not under examination. However, for the definition of typical crash scenarios, the study took advantage from the methodologies adopted for accident identification, reconstruction (Piantini et al., 2016) and potential avoidance.

The vehicle under study is based on the reproduction of the early CAD characteristics of the L2e-class demonstrator designed under the H2020 Resolve project (Resolve, 2018; Santucci et al., 2016). It is an in-line two-seater four wheel tilting vehicle, characterized by a maximum speed of 45 km/h (Bucchi et al., 2017); it has been proposed by Piaggio manufacturer. Considering that the analysis has been performed in a preliminary phase of the project in order to evaluate the overall crash solicitations on battery system, a known limitation of the study is that the CAD used for model reconstruction did not represent the final demonstrator vehicle. The prototypes presented at the end of the project itself, therefore, differ from the presented model due to the improvements which have been performed during vehicle development subsequent to this analysis. Nevertheless, the version here presented (corresponding to a late 2016 design) is still comparable to the final one in terms of overall size, mass, bodywork dimension, suspension layout. Overall characteristics of the vehicle at the moment of the execution of the crash simulation are summarized in Table 1, while the CAD model of the prototype is represented in Fig. 1.

It has to be highlighted that the results requested at the moment of the activity were an overview on the solicitations on the battery compartment, starting from the as-is configuration; known opportunities for vehicle improvement, not examined in the present document, include the assessment of solicitations on passengers and the optimization of vehicle design using sensitivity analysis on the basis of DOE methodologies, which is a way to fully exploit the potential of crash simulation methods (Barbani et al., 2014a).

Table 1. Summary of vehicle characteristics

Attribute	Value
Vehicle Class	L2e
Size	Compact
Target Mass (vehicle only, running order)	225 kg
Layout	4 wheel, tilting
Body type	Two seater, in-line
Maximum speed	45 km/h (12.5 m/s)
Battery type	2x 2kWh units, removable
Cell type	18650 format



Fig. 1. Prototype vehicle CAD model.

### 2.1. Accident scenarios selected for the vehicle under study

The selection of relevant accident scenarios has been made accordingly to the suggestions of manufacturers involved in the project and taking into account relevant scenarios as described by applicable technical documentation (ISO1323, 2005). The final selection included four crash configurations:

- Frontal crash test against rigid barrier
- Vehicle against car, crash from behind: ISO13232, type 131
- Vehicle against car, side crash: ISO13232, type 143
- Vehicle against car, frontal crash: ISO13232, type 413

The vehicle against car configurations are depicted in Fig. 2.



Fig. 2. Crash scenarios for four-wheel tilting vehicle according to ISO13232.

The selection has been done on the basis of suitable studies (Grassi et al., 2018a; Penumaka et al., 2014) which ranked the frequency of occurrence of certain scenarios starting from historical data available in literature (e.g. MAIDS, Motorcycle Accidents In-Depth Study) and, in certain cases, directly acquired. The final choice has been done assuming that:

- The crash configuration should have been relevant for battery compartment solicitation
- The set of scenarios should cover at least 50% of potential crash occurrence
  - an estimation based on the data provided by literature (Piantini et al., 2016) suggests that the value has been reached.

Vehicle speed at the crash instant has been assumed 10 m/s, that is 80% of maximum vehicle speed.

## 2.2. Preliminary identification of solicitation to be assessed on battery compartment

The results expected from the analysis comprehend a range of values, main being the acceleration on battery body, the solicitations on fixing points, the deformation in case of interference or penetration of external bodies in the volume of the battery. To acquire a preliminary set of reference values for the interpretation of results, a literature research on so-called abuse tests for battery cells to be used in electric vehicles has been done. The reference data provided by technical standards include accelerations comprehended in the range from 50g up to 150g, depending on reference test standard and on cell size (see Table 2).

Table 2. Summary of relevant technical standards to be used for battery/cell abuse test. Adapted from (Kraus, 2011).

Mechanical Abuse	UN 38.3	SAE 2464	IEC-62660-2
Impact	9.1 kg weight from 610mm height on rod		
Crush		85%, hold 5 minutes, 50% Speed: 0.5-1mm/min	Force stop based criteria: 15% deformation 30% voltage drop 1000x mass Hold for 24h
Mechanical Shock	150g; 6ms (Cell Energy <150Wh) 50g; 11ms (Cell Energy >50Wh) 3 shocks per direction	150g; 6ms (Cell Energy <150Wh) 50g; 11ms (Cell Energy >50Wh) 3 shocks per direction	50g; 6ms 10 shocks per direction
Vibration	Sine, 7 to 200Hz 3h per axis		Random, 10 to 2000 Hz 8h per axis
Penetration		3mm diameter 8cm/s Through cell	

For small cells such as those used for the vehicle under study (energy cell below 150Wh), SAE2464 describes the possibility to test up to 150g for 6ms, in all the directions and repeating shocks for 3 times. These values will be used for results interpretation.

The execution of virtual crash test since the beginning of vehicle development process through FEM simulations of motorcycle to car crashes represents a way to reduce costs and time (Barbani et al., 2014b) before executing real world crash test. For the vehicle under study, the execution of real-world test on the final product has not been performed, since the final prototype has been modified in comparison with the presented one.

### 3. Vehicle modeling activities

The vehicle model for the prototype can be divided in 4 different structure types, each one being related to the characteristics of the subsystem considered:

- Frame structure: thin walled tubes and metal sheets
- Suspension and wheels: solid metal components with undetermined degrees of freedom
- Electrical components: cables and solid components of various materials
- Body panels: mainly thin-walled polymer components

This section describes the modeling approach and the hypotheses assumed for the preparation of the model starting from vehicle geometry.

#### 3.1. Geometry adaptation for FEM analysis

The CAD geometry of the frame structure provided by the designer of the vehicle was composed of a disconnected parametric solid model, suitable for rendering and extraction of construction drafting. Based on this geometry, a shell surface model had to be reconstructed (semi-manually) in order to create a shell based FEM model for the crash simulation. Fig. 3 gives an overview on the modeling steps from a solid model to a shell discretization of the geometry.

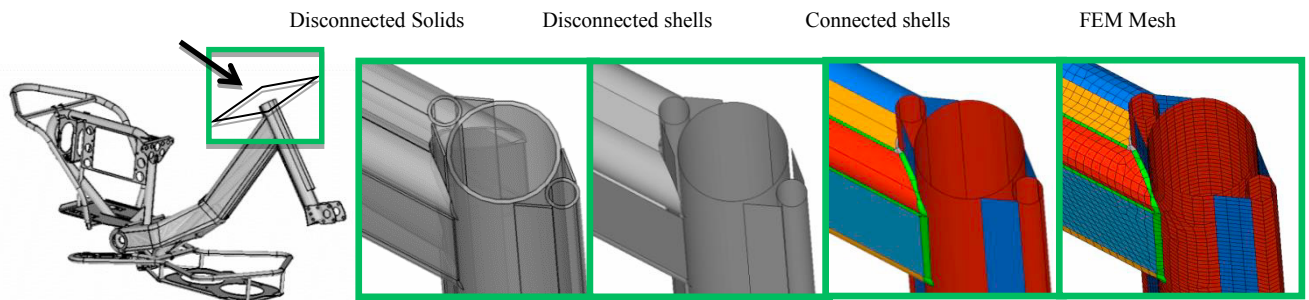


Fig. 3. Schematic overview on the modeling steps from a solid geometry to a FEM mesh.

In FEM simulation with explicit time integration the computation time is inversely proportional to the size of the maximum permissible step. The simulation time step has to satisfy the Courant-Friedrichs-Lewy (CFL) stability condition (Lewy et al., 1928), which is related to the geometry and size of the elements ( $L_{crit}$ ) and the corresponding dilatational wave propagation speed in the material model according to equation 1:

$$\Delta t_{CFL} = \frac{L_{crit}}{c} \quad (1)$$

where the compressive wave speed  $c$  in the medium/material depends on the elastic properties ( $E, \nu$ ) and specific density  $\rho$  as in equation. 2:

$$c = \sqrt{\frac{E(1-\nu)}{(1+\nu)(1-2\nu)\rho}} \quad (2)$$

The maximum permissible time step of the full model depends on the smallest time step related to the most critical element according to the described criteria. In practice this implies that very small elements should be avoided. Therefore, the trade-off need between modeling accuracy and computational cost needs to be considered. Such trade-off is particular relevant in case of structure optimization – an issue which requires the comparison of a large number of alternatives – and surrogate structures are needed to substitute full-detailed one (Sala et al., 2016); such approach has not been necessary for the system under study, since the proposed scenarios are suitable for direct solving in acceptable time according to the available calculation hardware.

### 3.2. Modeling of subsystems: frame, electrical system, suspensions

To model out-of-plane bending with plastic deformations components meshed with solid elements, a minimum of 2 quadratic elements trough the thickness in the direction of the bending plane is required to capture the non-linear plastic-strain field. Quadratic solid elements can however suffer from stability and accuracy issues due to negative Jacobians at quadrature points for problems involving large deformations (Belytschko et al., 2013). For components with large plastic out-of-plane deformations therefore, linear solids are used, in combination with mesh refinement. For thin-walled structures subjected to local bending deformations, shell elements with 5 integration points over the thickness<sup>1</sup> were used. For the motorcycle frame a typical in-plane shell element size of 5mm was used to model tubes and thin-walled components in the structure. Welding connections were either modeled by shell elements or local rigid beam elements connecting the elements of adjacent structures along the weld seam. For a relatively small number of elements with small critical lengths, local mass and or thickness scaling were applied, to avoid time-step limitations. Fig. 4 shows an overview with several details of the mesh of the frame structure.

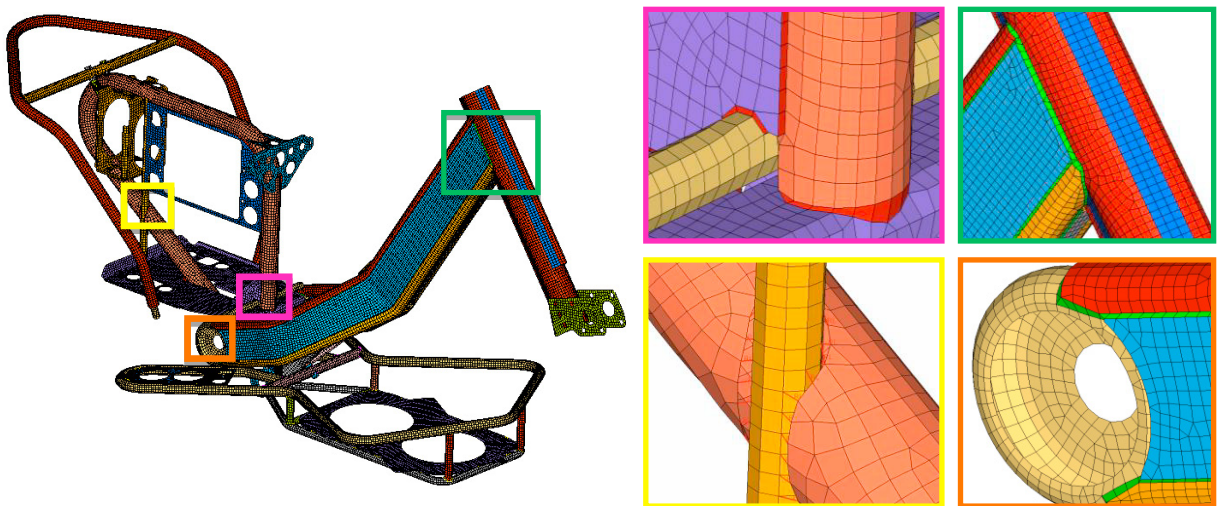


Fig. 4. Overview shell mesh of the motorcycle frame structure.

<sup>1</sup> An important advantage of shells over solid elements in the case of fracture due bending deformation is the possibility to apply Lobatto-Radau quadratures (see also (Abramowitz and Stegun, 1964; Ascher et al., 1995)) to assess the strain at the outer surface of the components where fracture typically initiates.



Many components of the motorcycle suspension and electrical components are voluminous to an extent that the shell assumption is inappropriate. These components were modeled using solid elements. Automatic tetra-meshing using Hypermesh v13 led to a high number of small elements, therefore mainly manual mapped Hex-meshing was used, while tetra-meshing was used only for a limited number of components characterized by irregular shapes and inconstant sections; in any case, the mesh has been manually checked and refined to avoid the risk of undesired elements. Hexahedron elements do not only perform better than tetra-elements in terms of critical element length but also in accuracy. Fig. 5 give an overview on some of the Hex-meshed solid components. Tyres – which are critical for correct crash assessment (Barbani et al., 2012) – are also included in the model.

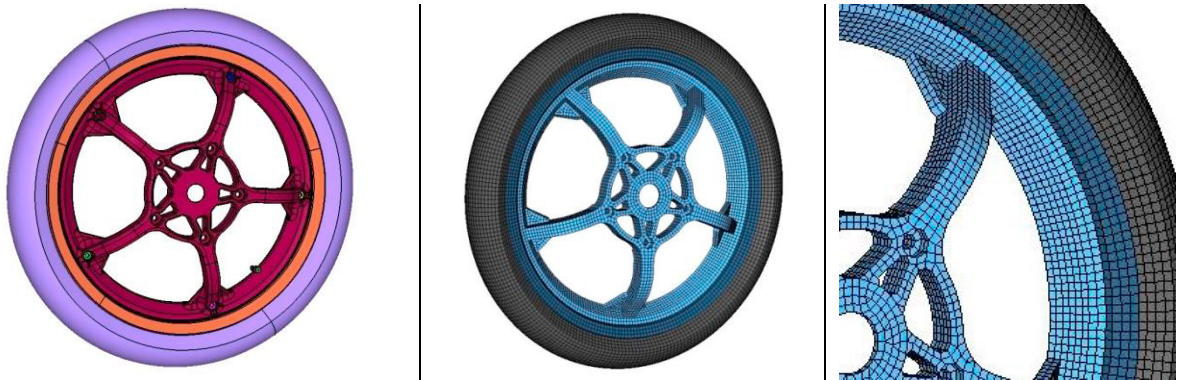


Fig. 5. Wheel assembly: comparison between CAD and FEM model and a detail on wheel spoke solid meshing.

Besides the elasto-plastic deformations of the motorcycle structure the dynamics and global deformation behavior of the motorcycle model are highly dependent on the kinematics of the motorcycle suspension. The springs, dampers, and kinematic constraints were approximated using 1 dimensional linear spring and damper elements and, where needed, setting cylindrical constraints to describe properly the functions of real vehicle joints, bearings and bushings. Fig. 6 gives an overview of the front suspension of the used FEM model.

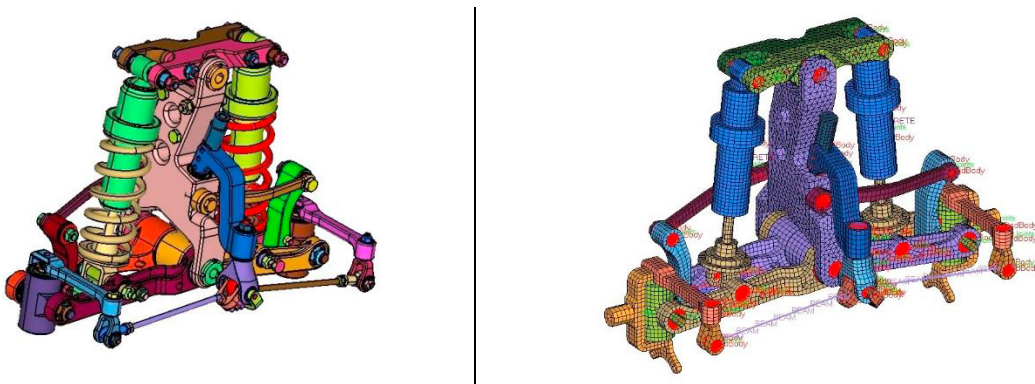


Fig. 6. Front suspension and steering system assembly: comparison between CAD and FEM models. Some components (e.g. steering links have been substituted by beam elements) have been simplified. For each bearing or constraint element, a proper functional constraint has been proposed.

The batteries were modeled using shell elements for the enclosure and structural interior reinforcements, and Hexahedron solid elements for the equivalent homogeneous block representing the cell stacks. Other electric components such as inverters and chargers were approximated by a combination of solid and shell elements. See Fig. 7 for an overview of the FEM representation of the batteries and inverter groups. These parts were modeled

with quite detail not only for their inertia characteristics but also due to their possible interaction with vehicle frame/subframe.

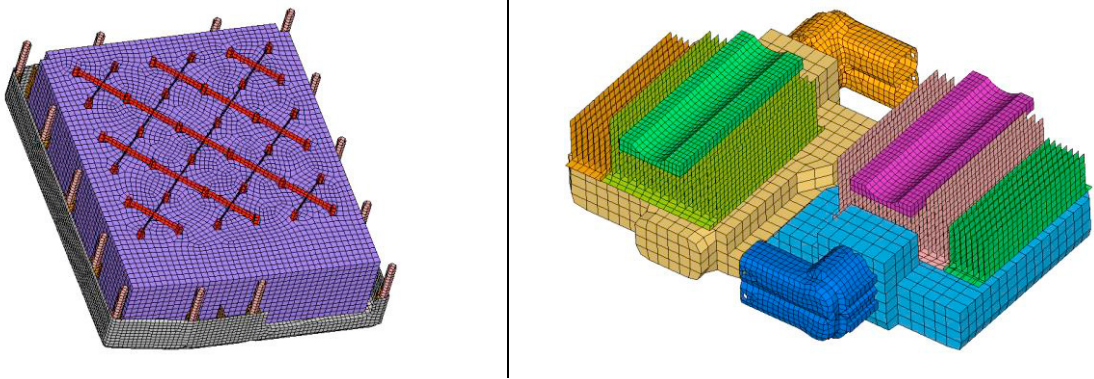


Fig. 7. FEM models of the battery casing (left) and inverter group (right).

Materials data, where available, have been provided by vehicle manufacturer. Main structural parts have been modelled using: Steel TSAR490 type; Steel C16 type (two different thermal treatments possible); ERGAL 7075 T6 type. For plastic parts, library suitable material model parameters were used according to the characteristics of the respective materials, such as ABS or PP.

### 3.3. Vehicle assembly

The L2e model structure, completed with various body elements, has been finally calibrated using additional mass distributed on the frame to reach the target value of 225kg; the resulting centre of mass is coherent with values obtained by the original CAD models. To merge all the components in the joined vehicle model, rigid body connectors were used to replace small elements such as fasteners, bolts and nuts etc.

Table 3 – Final characteristics of the mesh elements.

	L2e	Car	Dummy
Characteristics	nr [-]	nr [-]	nr [-]
Nodes	535774	283796	7444
Elements	582651	271504	4295
Elements 2D (Shell)	288965	267844	1636
Elements 3D (SOLID)	291214	2852	2648
Elements 1D (connectors)	2472	808	11
Components	255	340	116
Explicit time integration time step		4.5e-7 [s]	
Added mass (mass scaling)		0.896g] (<1% of L2e mass)	

To represent the influence of the rider on the kinetic impulse and crash dynamics during the simulation the HIII-50% Middle Adult male crash dummy model was included. The dummy model has a height of 175 cm, and mass of



78kg and was prepared and is supplied by the Livermore Software Technology Corporation<sup>2</sup>. Because the focus of the presented investigations is on the vehicle structure and batteries, no injury criteria of the dummy model are evaluated, and therefore the dummy model is not included in the post processing pictures.

Finally, the model has been subjected to the four crash scenarios described in paragraph 2.1. For the crash scenarios in which the L2e interacts with an automotive vehicle, the chosen vehicle is a Chrysler/Dodge Neon, a vehicle comparable to European C-segment and therefore being representative for the context of use. The Chrysler Neon Finite Element Model was taken from the finite publicly available element model archive of the National Crash Analysis Center<sup>3</sup>. An overview of the overall simulation model information of the L2e, dummy and impact vehicle is given in Table 3.

#### 4. Crash simulation results

The vehicle model, built as described, has been subjected to the four crash scenarios introduced in paragraph 2.1. Vehicle initial speed values are listed in Table 4.

Table 4 – Summary of initial conditions for the three simulation.

Scenario 1 – Rigid wall	Scenario 2 – type 143	Scenario 3 – type 131	Scenario 4 – type 413
L2e speed: 10 m/s	L2e speed: 0 m/s Car speed: 10 m/s	L2e speed: 0 m/s Car speed: 10 m/s	L2e speed: 10 m/s Car speed: 6.7 m/s

##### 4.1. Structural integrity

The results of the simulation for the case study of frontal impact with rigid wall are shown in Fig. 8, in the form of full vehicle frames extracted from crash animation. For this application, immediately after the contact between wheels and wall a plastic deformation begin on the frame, near to the head tube; other deformations are localized on various parts of the front suspension subassembly, and some components get fractured in consequence of energy absorption.

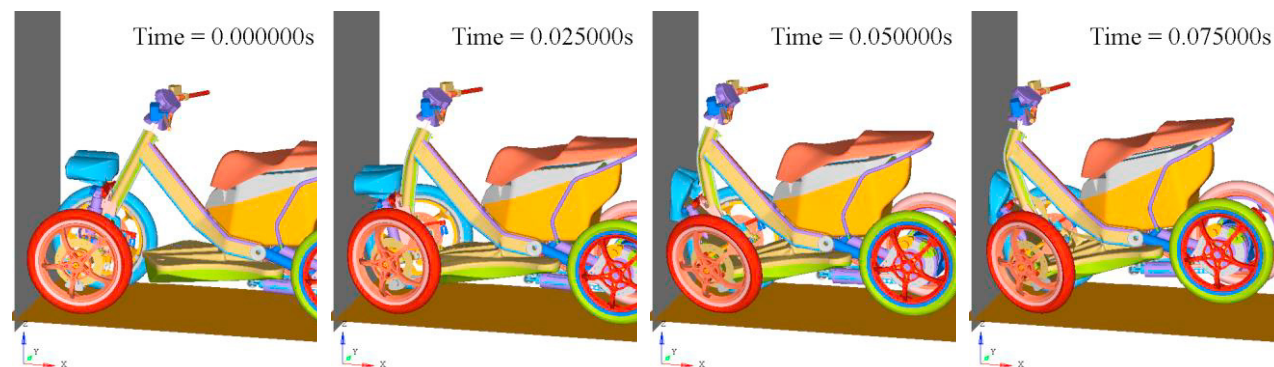


Fig. 8. Animation frame extracted from the simulation of the frontal impact of L2e demonstrator against rigid wall. Vehicle initial speed: 10m/s. The frames are comprehended in the range 0.01 - 0.075 s, total simulation time is 0.1s.

<sup>2</sup> [LSTC] Livermore Software Technology Corporation Dummy and Barrier Models for LS-DYNA  
[http://www.lstc.com/download/dummy\\_and\\_barrier\\_models](http://www.lstc.com/download/dummy_and_barrier_models) (retrieved February 2017)

<sup>3</sup> [NCAC] Finite Element model archive, These models have been developed by The National Crash Analysis Center (NCAC) of The George Washington University under a contract with the FHWA and NHTSA of the US DOT"  
<http://web.archive.org/web/20160408180243/http://www.ncac.gwu.edu/vml/models.html> (retrieved 8 April 2016).

The deformation causes the front vehicle suspension/tilting system to move in the direction of the footrest, absorbing energy until it interferes with the lower part of the footrest sub-frame. At this timestep, the remaining kinetic energy is reduced to less than 50% of the initial value. Further energy is absorbed in the subsequent deformation of steering head and footrest sub-frame; however, large part of the upper surface of the footrest remains free from external intrusions. Regarding the effect of vehicle crash on the battery, main point of interest used for the output calculation are the vehicle centre of mass and the centre of mass of each battery (right and left).

Fig. 9 shows the accelerations on selected points in case of frontal impact against rigid wall; the maximum value does not exceed 50g; local maximums are localized in case of initial impact (0.01s) and immediately after 0.05s, in consequence of the beginning of deformation of the footrest subframe. Energetic results are shown in Fig. 10, showing that main energy transfer is concluded before 0.1s, that is the end of the simulation.

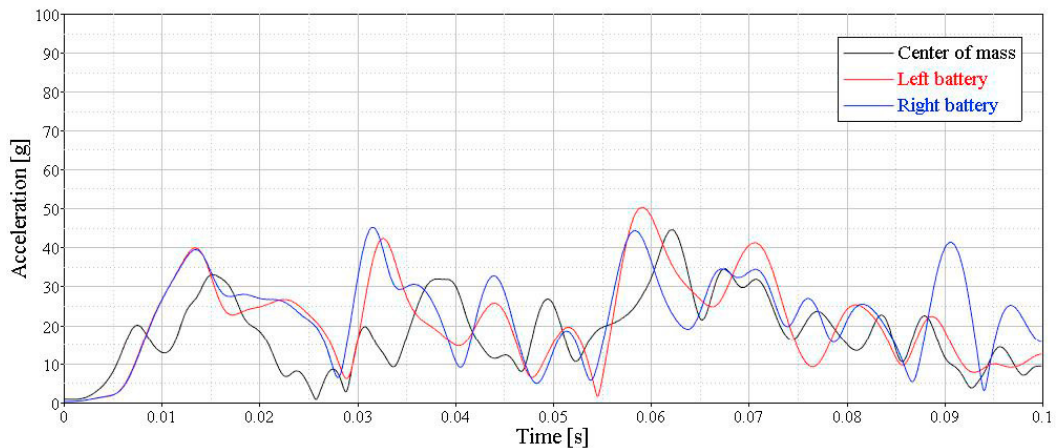


Fig. 9. Acceleration on vehicle centre of mass and of battery centres of mass in case of frontal impact against rigid wall.

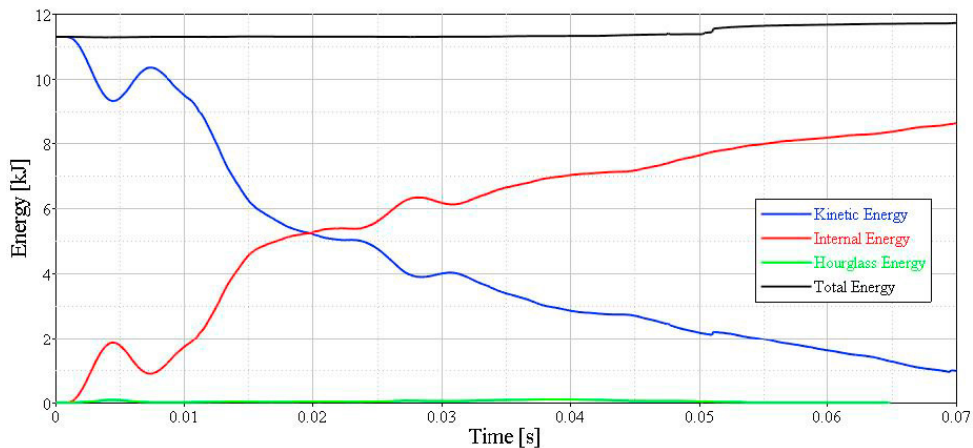






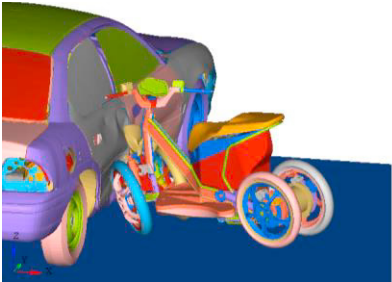


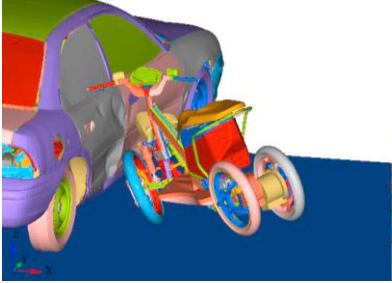
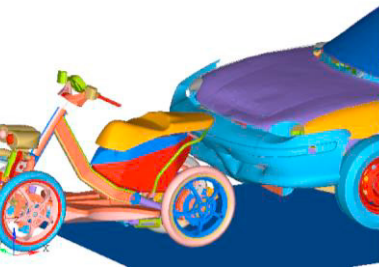
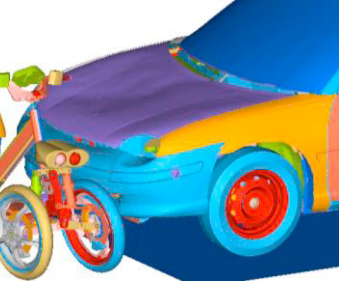
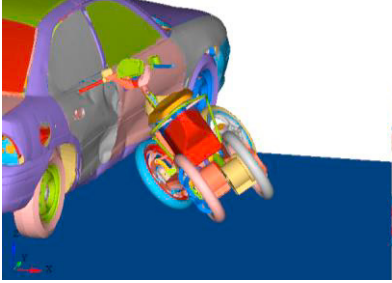
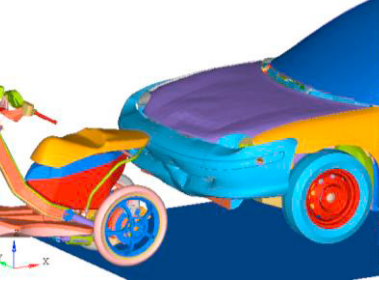
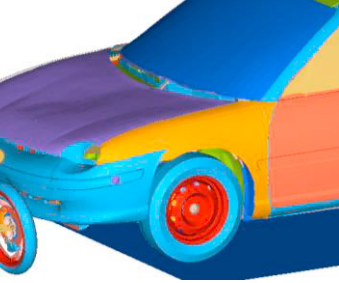


Fig. 10. Energy plot for the simulation shown in Fig. 8. Animation frame extracted from the simulation of the frontal impact of L2e demonstrator against rigid wall. Vehicle initial speed: 10m/s. The frames are comprehended in the range 0.01 - 0.075 s, total simulation time is 0.1s. The whole initial energy of the system corresponds to initial kinetic energy at 10m/s speed.

Considering other scenarios, the main results of the simulations are shown in Table 5, in the form of full vehicle graphics. Selected frames include simulation phase from 0 to 0.2 s.

Table 5. Comparison of crash scenarios in the 0-0.2s time interval. Rider is hidden for better representation..

	413 scenario	131 scenario	right 143 scenario
Time : 0.00s			
Time : 0.05s			
Time : 0.01s			
Time : 0.15s			
Time : 0.20s			

#### 4.2. Battery solicitations analysis

The results of frontal impact of the L2e vehicle against deformable car side implies the deformation of the front suspension system and of vehicle frame similarly to the impact on rigid wall, but the entity is reduced in such a way that the footrest is only slightly affected by intrusion. After the impact, the vehicle rotates due to the transversal speed induced by the contact with the moving car. Fig. 11 shows a maximum acceleration comparable with Fig. 9 in the first crash phase (0.05s). In case of impact of the car against L2e rear, the car bumper gets in contact with rear wheels and with the subframe under the seat; the impact implies the transfer of energy from such parts to the frame of vehicle, substantially protecting the seat and the battery compartment from deformation. The resulting accelerations are shown in Fig. 12. Also in this case, peak values on battery centre of gravity are below 40g. In case of impact of the car on the side of L2e, the contact initiates on both front and rear wheels of the vehicle, which are thus protecting the footrest of the vehicle. The consequence is a deformation of suspension elements assembly, while the vehicle is subject to lateral slide. Fig. 13 shows a peak value of about 100g.

In conclusion, in none of the scenario proposed the acceleration on battery system is estimated to be above the limits suggested by Table 2.

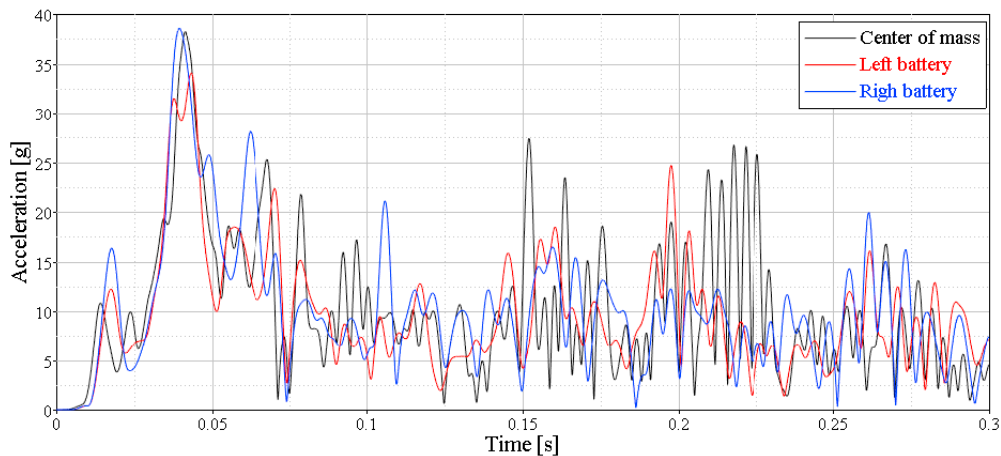


Fig. 11. Acceleration on vehicle centre of mass and of battery centres of mass in case of frontal impact against deformable car side (413 scenario).

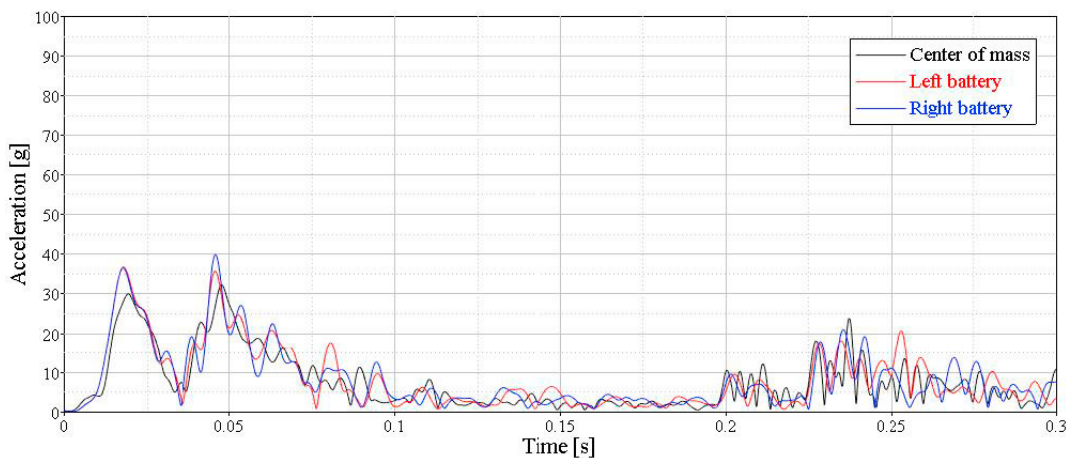


Fig. 12. Acceleration on vehicle centre of mass and of battery centres of mass in case of rear impact against deformable car (131 scenario).



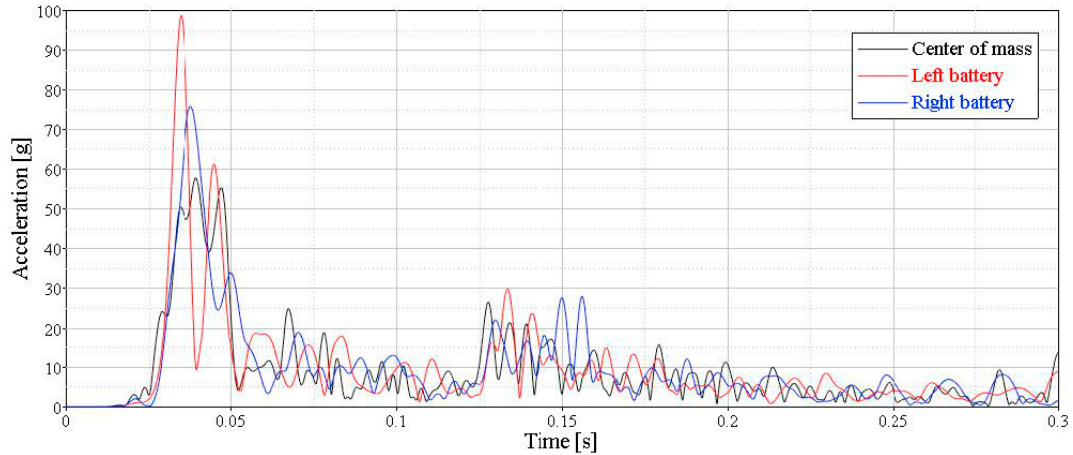


Fig. 13. Acceleration on vehicle centre of mass and of battery centres of mass in case of lateral impact against deformable car (143 scenario).

The consequences of the impact on the battery compartment have been studied considering additional parameters in comparison with other vehicle parts. An array of points disposed on the surface of battery casing have been selected and used to estimate the deflection of the case in comparison with edge points. Each scenario is described showing the equivalent stress on the battery surfaces and the deflection (measured in mm) of the most solicited wall.

Frontal impact against rigid wall: according to the data shown in Fig. 14, maximum stress values are localized on the lower part of battery casing, in correspondence with battery connector. Intrusion/deflection of battery casing is shown in the rear face and, according to full crash animation, its entity is mainly related to inertial effect.

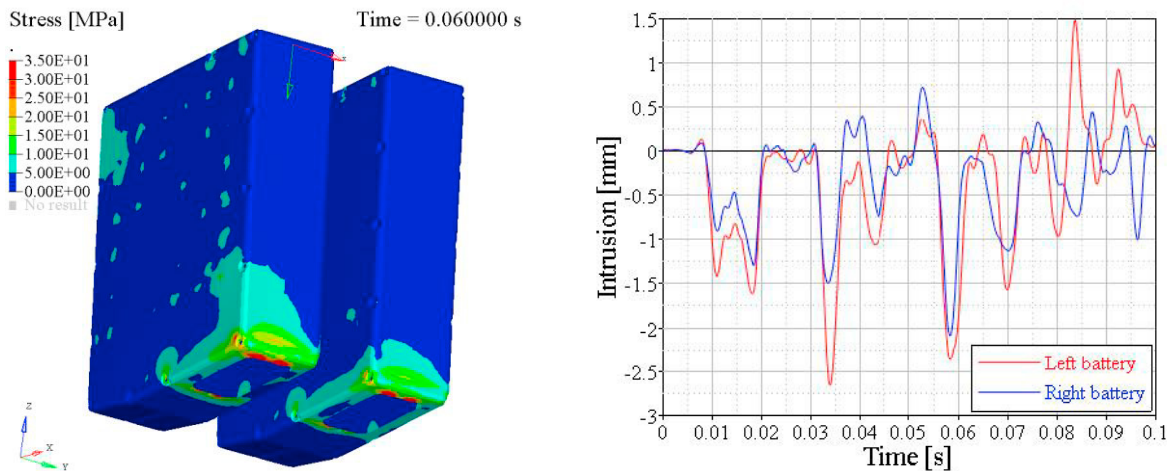


Fig. 14. Scenario: Frontal impact against rigid wall. Left: Battery casing stress (equivalent Von Mises stress). Right: intrusion/deflection of battery casing rear face (xy plane).

Frontal impact against deformable car side (413 scenario): according to the data shown in Fig. 15, maximum stress values are localized on the lower part of battery casing, in correspondence with battery connector. Intrusion/deflection of battery casing is shown in the rear face and, according to full crash animation, its entity is mainly related to inertial effects.



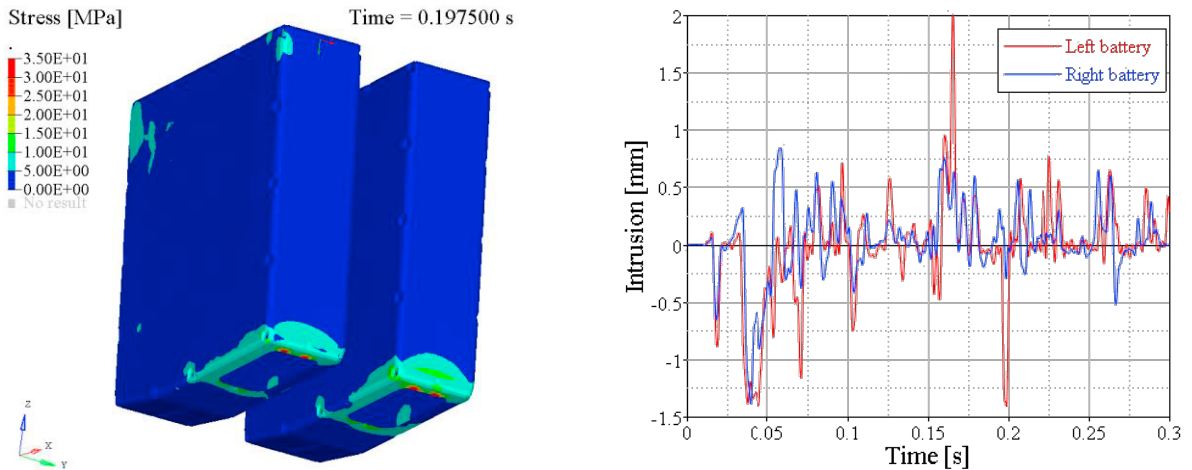


Fig. 15. Left: Battery casing stress (equivalent Von Mises). Right: intrusion/deflection of battery casing rear face (xy plane). Frontal impact against deformable car side (413 scenario)

Rear impact against deformable car (313 scenario): according to the data shown in Fig. 16, maximum stress values are localized on the lower part of battery casing, in correspondence with battery connector. Intrusion/deflection of battery casing is shown in the rear face and, according to full crash animation, its entity is mainly related to inertial effects.

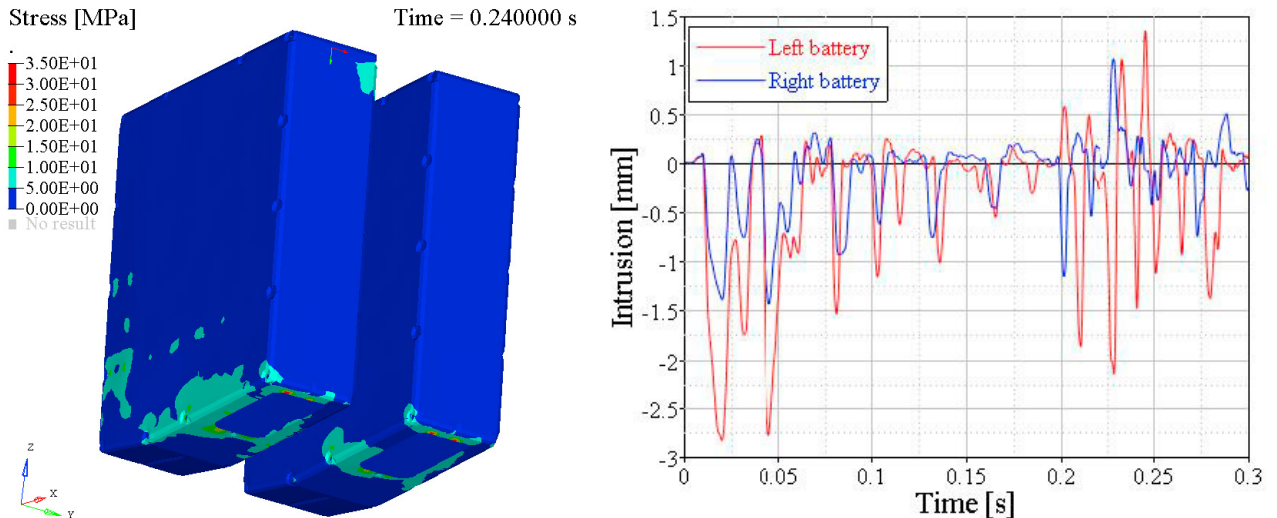


Fig. 16. Left: Battery casing stress (equivalent Von Mises). Right: intrusion/deflection of battery casing rear face (xy plane). Rear impact against deformable car (131 scenario).

Lateral impact against deformable car (143 scenario): the 143 scenario implies the contact of the incoming vehicle to the side of the L2e vehicle, and therefore is the most demanding case amongst those presented. According to the data shown in Fig. 17, maximum stress values are localized on the lower part of battery casing, in correspondence with battery connector and with underseat bodywork, this latter being in contact with the bumper of the incoming vehicle. Intrusion/deflection of battery casing is shown in such lateral face and, according to full crash animation, it is due to the contact with other vehicle bodywork parts.

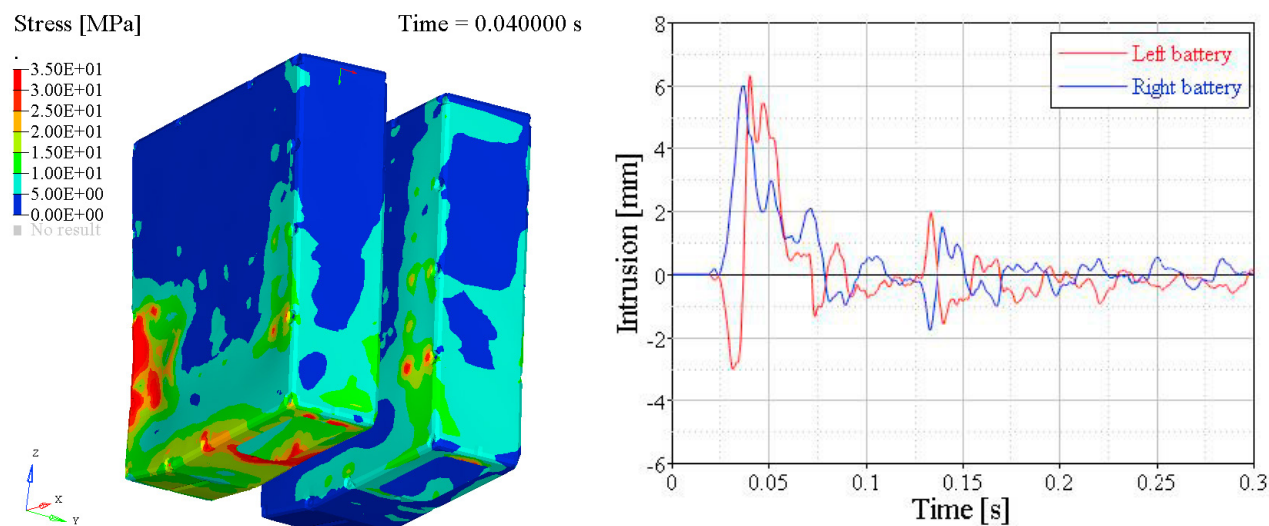


Fig. 17. Left: Battery casing stress (equivalent Von Mises). Right: intrusion/deflection of battery casing lateral face (zy plane). Lateral impact against deformable car (143 scenario).

As a final observation, the deflection of battery surfaces is estimated to be about 6mm for the worst scenario proposed; however, in this case, it is determined by the contact with vehicle bodyworks part not characterized by sharp edges, so that penetration of external parts in the battery shell are considered improbable.

## Conclusion

The study here described deals with the crashworthiness of a light vehicle which is innovative due to its layout, its dynamics (four-wheel tilting vehicle) and its electric powertrain. According to the potential criticalities associated with the use of high-energy density battery systems, the study is focused on the estimation of the solicitations of the battery itself. According to this need, a few scenarios have been selected based on the analogy of the studied vehicle to ordinary category of powered two wheelers. Then, a brief examination of worldwide abuse testing methods provided the order of magnitude of the limit solicitations to which the battery cells can be subjected.

Then, a detailed model of the vehicle has been built according to the detailed CAD and material information available from the manufacturer. Since the model was not used for the optimization of the vehicle, its level of detail is quite high and comprehends all the subsystems composing the vehicle.

The results of the simulation can be used to evaluate the overall behaviour of vehicle structure; focusing on the energy storage system – which was the initial object of the study – it is assessed that the acceleration on the battery centre of gravity falls within acceptable limits for all the case studies considered. In terms of material stress and overall deformation, the lateral crash is the most demanding scenario amongst those proposed; even in this case, the risk of penetration through battery surface is considered limited.

Considering the known limitations of the activity, future development of the study should include the thorough examination of worldwide regulation and testing procedures in order to ensure that the most demanding scenarios are selected for crash simulation, the improvement of battery submodel (e.g. including internal elements such as cells, spaces, conductors) and, where possible, the validation of the results using real-world crash measurements.

## Acknowledgements

The study was performed in relation to the RESOLVE project (Range of Electric Solutions for L-category Vehicles), a three years research project co-funded by the European Commission within the H2020 program (Call: H2020-GV-2014, Grant Agreement No 653511).

The authors gratefully acknowledge Piaggio & C. Spa of Pontedera (PI, Italy) for the technical support provided.

## References

- Abramowitz, M. (editor), Stegun, I.A. (editor), 1964. Handbook of mathematical functions with formulas, graphs, and mathematical tables. U.S. Department of Commerce, National Bureau of Standards.
- Ascher, U., Mattheij, R., Russell, R., 1995. Numerical Solution of Boundary Value Problems for Ordinary Differential Equations, Classics in Applied Mathematics. Society for Industrial and Applied Mathematics.
- Avdeev, I., Gilaki, M., 2014. Structural analysis and experimental characterization of cylindrical lithium-ion battery cells subject to lateral impact. *Journal of Power Sources* 271, 382–391.
- Barbani, D., Baldanzini, N., Pierini, M., 2014a. Sensitivity Analysis of a FE Model for Motorcycle-Car Full-Scale Crash Test (SAE Technical Paper No. 2014-32-0023). SAE International, Warrendale, PA.
- Barbani, D., Baldanzini, N., Pierini, M., 2014b. Development and validation of an FE model for motorcycle-car crash test simulations. *International Journal of Crashworthiness* 19, 244–263.
- Barbani, D., Pierini, M., Baldanzini, N., 2012. FE modelling of a motorcycle tyre for full-scale crash simulations. *International Journal of Crashworthiness* 17, 309–318.
- Belytschko, T., Liu, W.K., Moran, B., Elkhodary, K., 2013. Nonlinear Finite Elements for Continua and Structures. John Wiley & Sons.
- Bucchi, F., Cerù, F., Frendo, F., 2017. Stability analysis of a novel four-wheeled motorcycle in straight running. *Meccanica* 52, 2603–2613.
- Cahill, E., Taylor, B., Sperling, D., 2013. Low-Mass Urban Microcars for the Emerging Vehicle Markets of Megacities. *Transportation Research Record: Journal of the Transportation Research Board* 2394, 30–37.
- Cossalter, V., Doria, A., Ferrari, M., 2012. Potentialities of a Light Three-Wheeled Vehicle for Sustainable Mobility. Presented at the ASME 2012 International Design Engineering Technical Conferences and Computers and Information in Engineering Conference, American Society of Mechanical Engineers, pp. 523–532.
- Festini, A., Zenerino, A.T. and E., 2011. Urban and Extra Urban Vehicles: Re-Thinking the Vehicle Design. *New Trends and Developments in Automotive System Engineering*, Marcello Chiaberge, IntechOpen, DOI: 10.5772/13445.
- Gil, G., Savino, G., Piantini, S., Baldanzini, N., Happee, R., Pierini, M., 2017. Are automatic systems the future of motorcycle safety? A novel methodology to prioritize potential safety solutions based on their projected effectiveness. *Traffic Injury Prevention* 18, 877–885.
- Giovannini, F., Baldanzini, N., Pierini, M., 2014. Development of a Fall Detection Algorithm for Powered Two Wheelers Application (SAE Technical Paper No. 2014-32-0022). SAE International, Warrendale, PA.
- Grassi, A., Baldanzini, N., Barbani, D., Pierini, M., 2018a. A comparative analysis of MAIDS and ISO13232 databases for the identification of the most representative impact scenarios for powered two-wheelers in Europe. *Traffic Injury Prevention* 0 (in press), 1–24. <https://doi.org/10.1080/15389588.2018.1497791>
- Grassi, A., Barbani, D., Baldanzini, N., Barbieri, R., Pierini, M., 2018b. Belted Safety Jacket: a new concept in Powered Two-Wheeler passive safety. *Procedia Structural Integrity, AIAS2017 - 46th Conference on Stress Analysis and Mechanical Engineering Design*, 6-9 September 2017, Pisa, Italy 8, 573–593.
- Huertas-Leyva, P., Dozza, M., Baldanzini, N., 2018. Investigating cycling kinematics and braking maneuvers in the real world: e-bikes make cyclists move faster, brake harder, and experience new conflicts. *Transportation Research Part F: Traffic Psychology and Behaviour* 54, 211–222.
- ISO1323, 2005. ISO 13232-2:2005 - Motorcycles -- Test and analysis procedures for research evaluation of rider crash protective devices fitted to motorcycles -- Part 2: Definition of impact conditions in relation to accident data.
- Kraus, A., 2011. E-mobility - Making the future safe, in: 2011 4th International Conference on Power Electronics Systems and Applications. Presented at the Energy Storage, IEEE, Hong Kong, China, pp. 1–3.
- Lewy, H., Friedrichs, K., Courant, R., 1928. Über die partiellen Differenzgleichungen der mathematischen Physik. *Mathematische Annalen* 100, 32–74.
- Penumaka, A.P., Savino, G., Baldanzini, N., Pierini, M., 2014. In-depth investigations of PTW-car accidents caused by human errors. *Safety Science* 68, 212–221.
- Piantini, S., Pierini, M., Delogu, M., Baldanzini, N., Franci, A., Mangini, M., Peris, A., 2016. Injury Analysis of Powered Two-Wheeler versus Other-Vehicle Urban Accidents. Presented at the International Research Council on Biomechanics of Injury (IRCOBI) 2016, Malaga, Spain, p. 14.
- Resolve, 2018. Resolve Project Website [WWW Document]. URL <http://www.resolve-project.eu/> (accessed 8.4.18).
- Sala, R., Baldanzini, N., Pierini, M., 2016. Representative surrogate problems as test functions for expensive simulators in multidisciplinary design optimization of vehicle structures. *Structural and Multidisciplinary Optimization* 54, 449–468.
- Santucci, M., Pieve, M., Pierini, M., 2016. Electric L-category Vehicles for Smart Urban Mobility. *Transportation Research Procedia, Transport Research Arena TRA2016* 14, 3651–3660.
- Savino, G., Giovannini, F., Fitzharris, M., Pierini, M., 2016. Inevitable Collision States for Motorcycle-to-Car Collision Scenarios. *IEEE Transactions on Intelligent Transportation Systems* 17, 2563–2573.
- Will, F., Davdison, J.N., Couchman, P., Bednall, D., 2011. Tomorrow's Car - For Today's People: Can Tilting Three Wheeled Vehicles be a Solution for the Problems of Today and the Future? (SAE Technical Paper No. 2011-28-0001). SAE International, Warrendale, PA.
- Zhu, J., Wierzbicki, T., Li, W., 2018. A review of safety-focused mechanical modeling of commercial lithium-ion batteries. *Journal of Power Sources* 378, 153–168.